Designing Material Properties Locally with Additive Manufacturing technology SLM

A.B. Spierings, K. Wegener†, G. Levy**

* INSPIRE AG – institute for rapid product development irpd, Lerchenfeldstrasse 5, CH-9014 St.Gallen, Switzerland

† ETH Zürich, Institut für Werkzeugmaschinen und Fertigungstechnik (IWF), Tannenstrasse 3, CH-8092 Zurich, Switzerland

REVIEWED, Accepted August 16, 2012

Abstract

Additive Manufacturing technologies are known to allow the production of parts with an extreme degree of complexity, enabling design and functional part optimization. So far the development of processing parameters and analyze of corresponding materials focuses on dense materials for maximized material properties. However, AM processes like Selective Laser Melting, allow also the generation of materials with some degree of porosity affecting their mechanical properties. A DOE was set up for SLM processed SS 17-4PH / AISI-630 material with porosity between 0% and about 26% in order to analyze mechanical properties. The results presented show that the porosity significantly affects material ductility and hardness, offering the possibility to design a material according to the required mechanical behavior of the parts produced. Therefore, this AM enabling features allows a multi-property component design by appropriate local parameter setting.

Keywords:
Additive Manufacturing, Selective Laser Melting, stainless steel, material properties

---

I. Introduction

Additive Manufacturing Technologies offer many advantages for the tool-less production of highly complex structured parts directly from CAD data. Especially the Selective Laser Melting (SLM) Technology, a powder-bed based process, allows the production of parts in a wide range of metallic materials by selectively fusing a metallic powder material. Thereby, the remaining part-porosity can be kept below 1% by choosing appropriate processing parameters. The resulting static mechanical properties are typically widely comparable to values from conventionally processed materials, e.g. for stainless and hot-work steel [1, 2], Aluminium [3-5], Titanium [6], Ni-based materials [7, 8]. Consequently, such parts can be used in a wide field of industrial applications: Tooling industry, lightweight structures for automotive and aerospace, functionally optimized parts for diverse industrial and customized implants and instruments for medical applications.

The SLM process uses a high power Nd-YAG laser source in order to continuously create side by side scan tracks filling the successive cross-sections of the parts to be produced. The main processing parameters are therefore the power of the laser source, the scan velocity, the hatch distance of the laser scan tracks and the thickness of the powder layers to be scanned [9]. An almost densely processed material can be reached for the successful selection of a suitable set of these processing parameters. Typically, there is not only one possible set of processing parameters for a given material, but several different combinations.

Design of Experiment (DOE) techniques are therefore useful to analyse the significance of the different processing parameters and to select suitable combinations for a given target value. Different researchers have used DOE in order to analyse the SLM-process and its parameters. Chatterjee [10] used a central composite design to analyse the effect of the main processing parameters on the part density / porosity and the hardness of a M2 work steel. Liao [11] used DOE to select an optimal processing parameter sets for achieving minimal porosity for nickel material. Averyanova [12] used a fractional factorial design to identify an optimal set of processing parameters for single laser tracks from stainless steel 17-4PH. They successfully identified the impact of the same processing parameters as mentioned above on the width, the height and the contact angle of the scan tracks as well as the roughness and geometrical characteristics of a single fused layer.

Such previous work aimed primarily on optimal processing parameters for dense material [1, 2, 11-13] or on the properties of lattice structures [14, 15]. However, as AM Techniques are master forming technologies [16], not only the macroscopic geometrical structure but also the material itself with its properties are defined by the process. Therefore, by adjusting processing parameters, a desired degree of porosity can be generated affecting the mechanical properties of the material, e.g. its elasticity. The major effect of porosity on E-Modulus has been widely investigated and different models have been proposed [17-19].
Current work aims at investigating the possibilities for adjusting basic mechanical properties such as E-Modulus, hardness for a SLM manufactured stainless steel 17-4PH / AISI-630 material by using a full factorial DOE. The dependency of E-Modulus on porosity is validated against the model of Boccaccini [18]. The results show that adjustments of mechanical parameters are possible in a wide range, especially for hardened 17-4PH material.
This offers the opportunity to locally design the mechanical behaviour of a structure not only by its geometrical design, but also by adjusting the material porosity.

II. Methods and Materials

a) SLM Machine and Materials

The SLM machine type Concept Laser M2 was used, which is equipped with a Nd:YAG fiber laser having a maximal laser power of about 190W at the build platform and a nominal laser spot diameter of about 0.1mm. The scan strategy used to produce the tensile samples is a chess-board like scanning structure with 5x5 mm^2-squares. More details are described in [20, 21].
A hardenable stainless steel 17-4PH / AISI-630 material was used for this study. The raw powder material had the characteristics according to Table 1, allowing a productive and high quality production at all layer thicknesses used (see Table 2) [2].

Table 1: Composition (%) and characteristics of the powder material used

Composition	Fe bal.	Cr 16.7	Ni 4.5	Cu 4.3	Si 0.4	CbTa 0.3	Mn 0.3	N 0.12	C 0.02
Powder	D_{10} = 16.4µm			D_{50} = 26.8µm			D_{90} = 42.7µm		

Half of the specimens were heat treated according to the following procedure: Annealing at 1350°C, solution heat treatment at 1050°C, subsequent deep freezing & ageing at 480°C / 1h (condition H925).

b) Design of Experiment

A full-factorial experimental design was chosen. The factors and corresponding levels are listed in Table 2. The levels were defined on the basis of the results of pre-trials.

Table 2: DOE factors and corresponding levels

		Level 1	Level 2
Build orientation	(-)	Vertical (90°)	Horizontal (0°)
Layer thickness t_{Layer}	(µm)	30	50
Scanning speed v_{Scan}	($^{mm}/_{s}$)	800	1300
Laser Power[1] P_{Laser}	(W)	105	190
Annealing	(-)	without	with

The Hatch distance was kept constant at 0.0975 mm (35% overlap of scan tracks). Cylindrical blanks for tensile test specimens (Figure 1) were produced with all combinations of above factors with 2 repetitions for each combination. Additionally, each combination was produced without and with heat treatment (annealing), resulting in total 96 specimens. The specimens where then drilled to the final geometry according to ISO/DIN 50'125-B4x20.

Figure 1: Tensile specimens (190W, 800$^{mm}/_{s}$) – horizontally produced blank (left) and final drilled specimen according to DIN-50125-form B (right).

Tensile testing was performed using a universal testing machine type Zwick-1484 with a pre-load of 20MPa and a testing speed of 10^{-3} s^{-1}. Brinell hardness measurements (HB 2,5/62,5) were performed at the end planes of the final tensile specimens. Therefore, for the horizontally built specimens, hardness was measured in parallel to the layers where as for the vertically build specimens, hardness was measured vertically to the layers.

III. Results

a) Material density

Density was measured on pre-manufactured cubes (10x10x10 mm^3) using the Archimedes method, offering good repeatability [22]. The energy density ($^J/_{mm^3}$) supplied to the powder layer was calculated according to equation 1 [23], taking into account laser power P_{Laser} (W), scan speed v_{scan} ($^{mm}/_s$), hatch distance h_s (mm) and powder layer thickness t_{Layer} (mm):

$$E-density = \frac{P_{Laser}}{v_{scan} \cdot h_s \cdot t_{Layer}} \quad (1)$$

Figure 2 shows the influence of the specific energy input into the powder layer on the resulting part density. Good curve fitting for a resulting part density >≈ 75% was obtained with equation 2, where a = $^1/_{E\text{-}Density}$ ($r^2 = 0.96$).

$$Density = 0.92 + 12.2 \cdot a - 514 \cdot a^2 + 4318 \cdot a^3 \quad (2)$$

Figure 3 shows exemplary the pore distribution and sizes for porous (left) and almost dense material. It can be noted that with insufficient energy input, the pores become larger and partially interconnected.

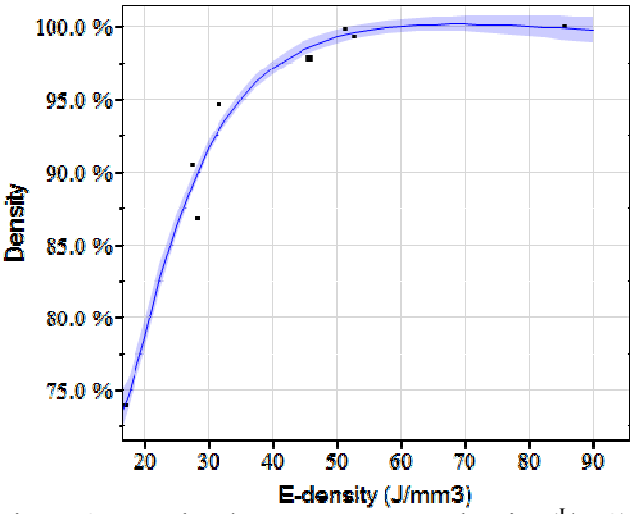

Figure 2: Part density versus Energy density ($^J/_{mm}3$). Confidence level 95%

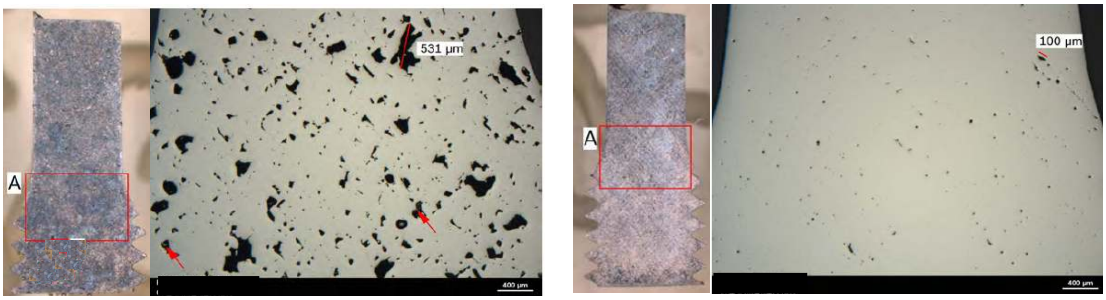

Figure 3: Micrographs, left: P_{Laser} = 190W, v_{Scan} = 1300$^{mm}/_s$, t_{Layer} = 50µm, right: P_{Laser} = 190W, v_{Scan} = 800$^{mm}/_s$, t_{Layer} = 30µm.

E-modulus, hardness and Yield strength

Literature values for the E-modulus for wrought 17-4PH material are between 197 – 207GPa (condition H925) [24]. The E-Modulus of the AM processed, heat treated 17-4PH material is highly comparable: For optimised density 199 GPa (horizontal) and 187 GPa (vertical), respectively. This difference between horizontal and vertical build orientation is about 5.7%; the absolute differences remain comparable over the whole density range (9.9 ± 2.9 GPa). Figure 4 shows that the modulus for heat treated material highly depends on the material density: Allowing a porosity of about 26%, E-modulus can be reduced to only ≈ $^1/_5$ of the maximal value.

In contrast, the modulus of the non-heat treated samples varies significantly around a mean value of ≈ 152 GPa and no significant trend in its relationship to porosity can be identified (Figure 4). The stiffness values for the 74% samples could not be measured accurately and they broke very early.

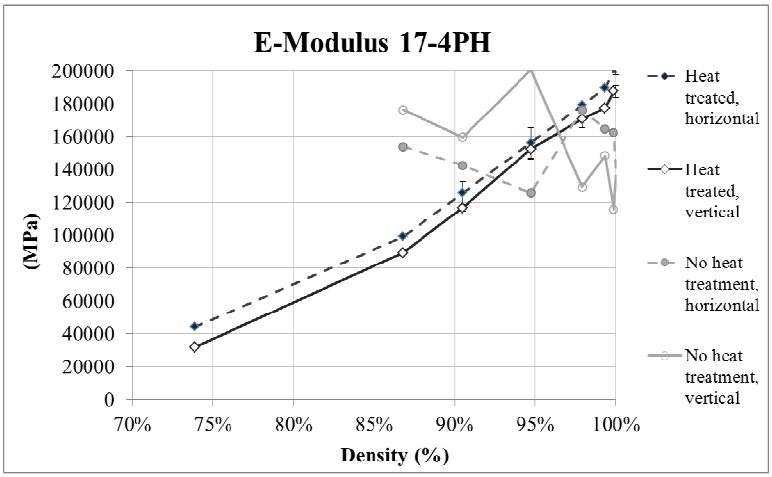

Figure 4: E-Modulus for heat treated and non-heat treated material versus density, vertical & horizontal build orientation

Hardness is also dependent on the material density for both heat treated and non-heat treated material (Figure 5). For dense, heat treated material, hardness values are within literature value ranges [24] and statistically not significantly different for horizontal or vertical build orientation, respectively (horizontal: HB 400 ± 1.6, vertical: HB 389 ± 16.3). For the non-heat treated material the maximal values are also almost identical (horizontal: HB 233, vertical: HB 235).

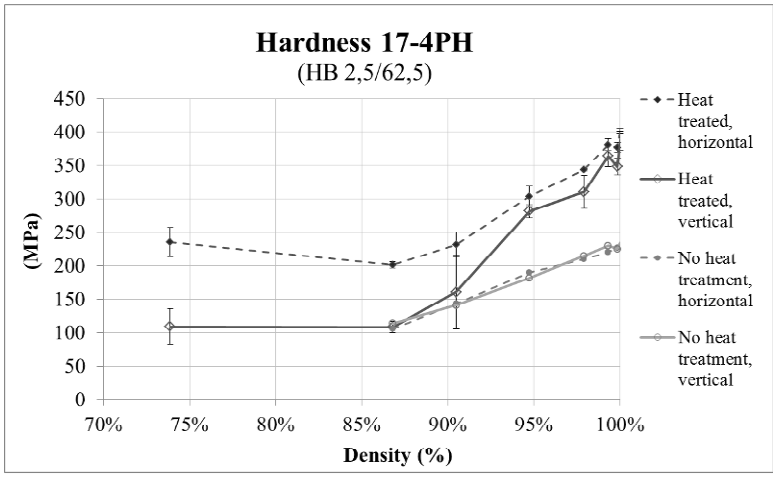

Figure 5: Hardness for heat treated and non-heat treated material versus density, vertical & horizontal build orientation

In addition to E-modulus and hardness, Yield strength shows a good correlation to density or applied energy density (see Figure 2), both in heat treated and non-heat treated condition. Differences between horizontal and vertical build orientations exist, but are not significant for the heat treated condition. However, in the as-built condition, differences can be observed and remain comparable over the whole analysed range (108 ± 41 MPa). This is a direct result of the dendritic microstructure having a long grain axis parallel to the z-axis (90° orientation) and can be understood by the well known Hall-petch relationship.

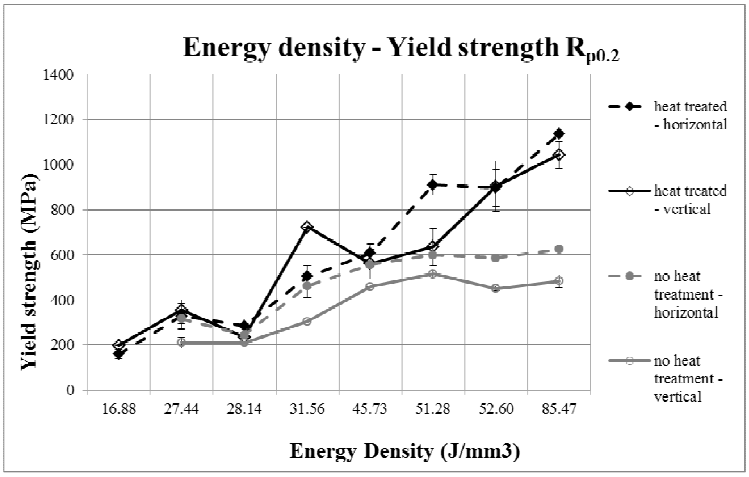

Figure 6: Yield strength - Energy density for heat treated and non-heat treated condition, vertical and horizontal build orientation

IV. Discussion

The energy density (equation 1) can be considered as the main driving parameter for material density. Presented data (Figure 2) are valid for all combinations of laser power, scan velocity and layer thickness according to Table 2. Therefore, no distinction is made between specific factor combinations and observations in subsequent presented results. The following discussions are focusing on heat treated 17-4PH material, as the results for the E-modulus (Figure 4) show a very good correlation to material density. Nevertheless, the basic behaviour of not heat treated material can be compared to the heat treated material, except for the E-modulus (Figure 4).

The dependency of E-modulus on material density, for both horizontal and vertical build orientation, can be described by a 2nd degree polynomial fit (equation 3, Figure 7).

$$\text{E-modulus} = -540952 + 730482 * \text{density} + 1037193 * (\text{density}-0.9371)^2 \quad (3)$$

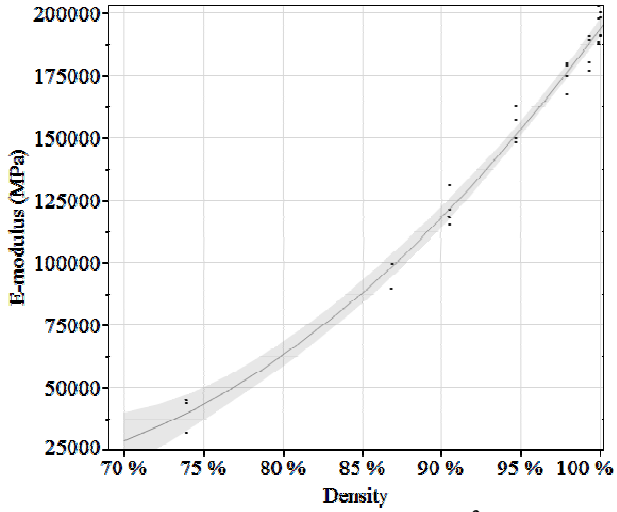

Figure 7: E-modulus with 2nd degree polynomial fit ($r^2 = 0.99$), 95% confidence interval for expected mean values

However, it is interesting to compare this porosity-dependent behaviour of E-modulus to commonly used mathematical models; Boccaccini [18] gives a good overview on a variety of different models. Typically, these models have been developed for other material classes (e.g. ceramics) and corresponding processing techniques. Most of the models assume spherical and homogeneously distributed pores of the same size. However, this is not true in most of the real cases. For AM processed materials, a more or less homogeneous pore distribution can be expected, especially at low porosity levels (Figure 3 right, [22]). At higher porosity levels, pores begin to be interconnected, which

is a result of the non-equilibrium process characteristics, leading to balling phenomena [25] of the scan tracks and insufficient melting of powder particles etc. Therefore, pores will not be of the same size nor spherical in shape (Figure 3, left).

Anyway, Figure 8 shows good correlation between caluclated and measured E-modulus using the formula presented by Baccaccini (equation 4), with P the material porosity (= 1 – density), E_M the E-modulus of the pore-free material and R the particle size ratio, used in this study as a curve fitting parameter, giving insight into a (theoretical) structure of the pores. The smaller the R-value, the smaller are the pores. Thus for a given porosity and a lower R-value, more but smaller pores are present in the material.

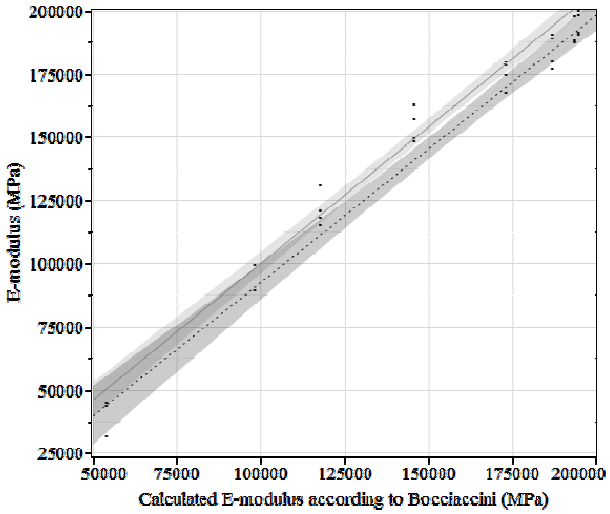

Figure 8: Caluclated (Bacciaccini [18]) versus measured E-modulus for horizontal (—) and vertical (--) build orientation with 95% confidence interval for expected mean values.

$$E_P = E_M \cdot \frac{(1-P)^2 \cdot R}{P+(1-P)\cdot R} \tag{4}$$

For E_M = 194.5 GPa (mean for horizontal and vertical build oritentation) and R = 0.21, a very good correlation can be found ($r^2_{vertical} = 0.98$, $r^2_{horizontal} = 0.99$), indicating general usability of conventional mathematical formalism for E-modulus. Boccaccini used R-values of 0.6 to 1.0 for ceramic materials, indicating bigger pores compared to AM processed materials.

Material hardness highly depends on density (Figure 5), both for heat treated and non-heat treated material. However, below a certain density (≈ 87%), hardness is not further reduced. This indicates that hardness is influenced by the pore structure and therefore by the deformation behaviour of the remaining material under pressure. Supposing isotropic material behaviour under tension and compression, the stiffness of this remaining material is affected by E-modulus for elastic deformation, and Yield strength for the beginning of plastic deformation. It is therefore reasonable to analyse hardness in relation to E-modulus and Yield strength (Figure 9). Detailed results on the dependency of Yield strength on material density is being presented in an upcoming publication.

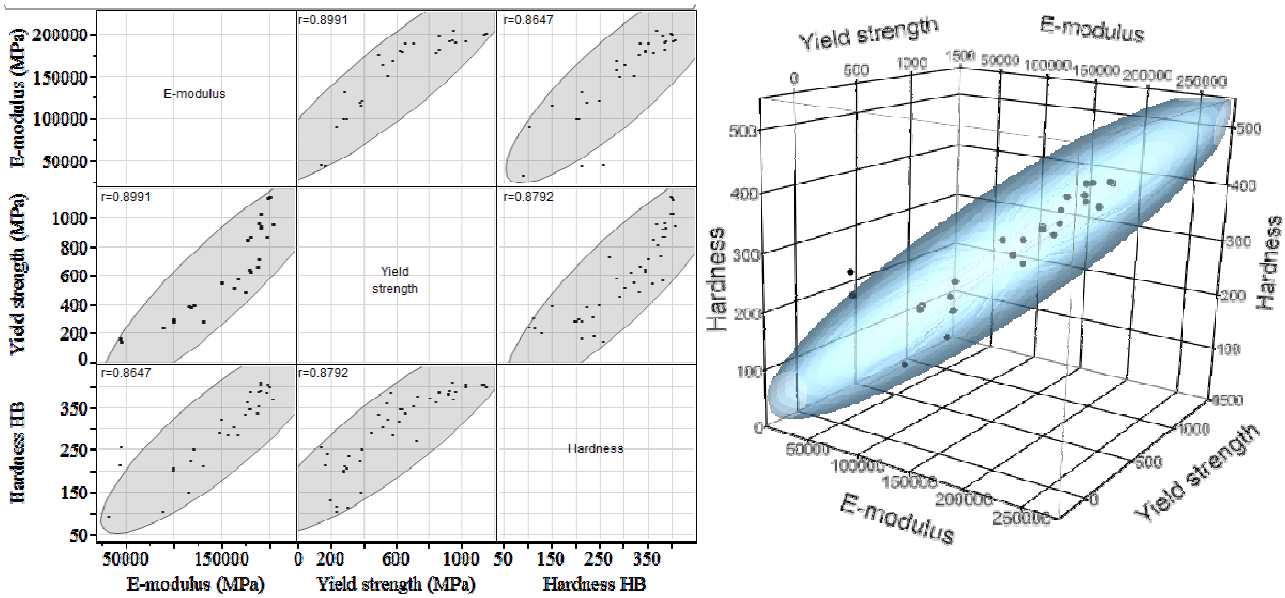

Figure 9: 95%-Density-Ellipse for Hardness (heat treated) in relation to E-modulus and Yield strength. R-values indicate correlations (restricted maximum likelihood method)

For heat-treated material, a correlation to both parameters is obvious. In contrast, as E-modulus for the non-heat treated material does not correlate with porosity (Figure 4), only a correlation to Yield strength can be observed (Figure 10).

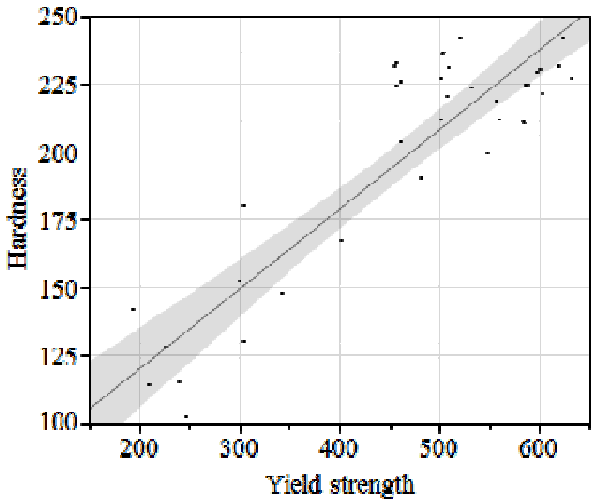

Figure 10: Hardness versus Yield strength (non-heat treated). 95% confidence interval, $R^2 = 0.80$

V. Conclusions

Selective Laser Melting allows not only the production of highly complex three dimensional parts. Its peculiarity of generating the material in the sense of a master forming technology allows also designing the mechanical material properties of the parts, e.g. the stiffness, by allowing a specific degree of porosity. The dependency of the E-modulus on porosity can be described by known mathematical formula, e.g. by Boccaccini [18]. It is expected that this formula is easily adaptable to other materials.

By a space-resolved adjusting of the relevant processing parameters, the results show that it is possible to locally design not only the structure but also the specific material behaviour. This allows optimizing the global mechanical part behaviour before the desired technical requirements of a part in service. It opens the way to functionally improved medical implants or instruments, and generally to a wide field of machine parts etc.

VI. Outlook

In this publication, only density-dependent results on the E-modulus and hardness are reported. Further results on the dependency of mechanical properties of material density, especially for Yield strength and Ultimate strength, are going to be published in a separate publication. Beside an analysis of 17-4PH material, other materials should be analysed in order to be able to transfer the possibilities of designing the mechanical behaviour of a structure into industry specific applications: Titanium, Aluminium, etc.

Complementary, the dependency of the dynamic mechanical properties on density should be analysed in more detail and correlated to existing formula for the dependency of fatigue behaviour on porosity.

Acknowledgements

The authors gratefully acknowledge Mr. A. Frauchiger for his support in the production of test specimens. We furthermore thank Dr. M. Schmid for his critical reading this paper.

Literature

1. Averyanova, M. and P. Bertrand. *Direct Manufacturing of dense parts from martensitic precipitation hardening steel gas atomized powder by Selective Laser Melting (SLM) technology*. in *Int. Conference on Advanced Research in Virtual and Rapid Prototyping*. 2010. Leiria, Portugal: CRC Press / Balkema.
2. Spierings, A.B., N. Herres, and G. Levy, *Influence of the particle size distribution on surface quality and mechanical properties in additive manufactured stainless steel parts.* Rapid Prototyping Journal, 2011. **17**(3): p. 195 - 202.
3. Berkau, A. *Einsatzmöglichkeiten des Strahlschmelzens zur Herstellung von Bauteilen aus Aluminium*. in *16. Anwenderforum Rapid Product Development*. 2011. Stuttgart: citim GmbH.
4. Brandl, E., et al., *Additive manufactured AlSi10Mg samples using Selective Laser Melting (SLM): Microstructure, high cycle fatigue, and fracture behavior.* Materials & Design, 2012. **34**(0): p. 159-169.
5. Buchbinder, D., et al., *High Power Selective Laser Melting (HP SLM) of Aluminum Parts.* Physics Procedia, 2011. **12, Part A**(0): p. 271-278.
6. Murr, L.E., et al., *Microstructure and mechanical behavior of Ti-6Al-4V produced by rapid-layer manufacturing, for biomedical applications.* Journal of the Mechanical Behavior of Biomedical Materials, 2009. **2**(1): p. 20-32.
7. Mumtaz, K.A., P. Erasenthiran, and N. Hopkinson, *High density selective laser melting of Waspaloy®.* Journal of Materials Processing Technology, 2008. **195**(1-3): p. 77-87.
8. Rickenbacher, L., et al., *High temperature material properties of IN738LC processed by Selective Laser Melting (SLM) technology.* Rapid Prototyping Journal, submitted.
9. Kruth, J.P., et al. *Rapid Manufacturing of Dental Prostheses by means of Selective Laser Sintering/Melting*. in *European Forum on Rapid Prototyping & Manufacturing AFPR*. 2005. Paris, France.
10. Chatterjee, A.N., et al., *An experimental design approach to selective laser sintering of low carbon steel.* Journal Of Materials Processing Technology, 2003. **136**(1-3): p. 151-157.
11. Liao, H.T. and J.R. Shie, *Optimization on selective laser sintering of metallic powder via design of experiments method.* Rapid Prototyping Journal, 2007. **13**(3): p. 156-162.
12. Averyanova, M., et al., *Experimental design approach to optimize selective laser melting of martensitic 17-4 PH powder: part I – single laser tracks and first layer.* Rapid Prototyping Journal, 2012. **18**(1): p. 28-37.
13. Vandenbroucke, B. and J.P. Kruth, *Selective Laser Melting of biocompatible metals for rapid manufacturing of medical parts.* Rapid Prototyping Journal, 2007. **13**(14): p. 196-203.
14. Parthasarathy, J., B. Starly, and S. Raman, *A design for the additive manufacture of functionally graded porous structures with tailored mechanical properties for biomedical applications.* Journal of Manufacturing Processes, 2011. **In Press, Corrected Proof**.
15. Rehme, O., *Selective Laser Melting offenzellulärer Strukturen und Charakterisierung ihrer mechanischen Eigenschafte* 2006, Institute of Laser and System Technologies: TU Hamburg-Harburg. p. 1-30.
16. DIN 8580, F.T.S.C., *Manufacturing processes - Terms and definitions, division*, in *DIN 8580*. 2003, DIN German Institute for Standardization. p. 13.

17. Arnold, M., A.R. Boccaccini, and G. Ondracek, *Prediction of the Poisson's ratio of porous materials.* Journal of Materials Science, 1996. **31**(6): p. 1643-1646.
18. Boccaccini, A.R. and Z. Fan, *A new approach for the Young's modulus-porosity correlation of ceramic materials.* Ceramics International, 1997. **23**(3): p. 239-245.
19. Chawla, N. and X. Deng, *Microstructure and mechanical behavior of porous sintered steels.* Materials Science and Engineering: A, 2005. **390**(1–2): p. 98-112.
20. Spierings, A.B. and G. Levy. *Comparison of density of stainless steel 316L parts produced with selective laser melting using different powder grades*. in *Proceedings of the Annual International Solid Freeform Fabrication Symposium*. 2009. Austin, Texas.
21. Badrosamay, M., et al. *Improving Productivity Rate in SLM of Commercial Steele Powders*. in *SME-RAPID*. 2009. Schaumburg, IL, USA.
22. Spierings, A.B., M. Schneider, and R. Eggenberger, *Comparison of Density Measurement Techniques for Additive Manufactured metallic Parts.* Rapid Prototyping Journal, 2011. **17**(5): p. 380-386.
23. Kruth, P.d.i.J.P., et al., *Rapid Manufacturing of Dental Prostheses by means of Selective Laser Sintering/Melting*, in *Proceedings of the AFPR, S4*. 2005.
24. GRANTA-software, *CES EduPack*. 2012.
25. Kruth, J.P., et al., *Selective laser melting of iron-based powder.* Journal Of Materials Processing Technology, 2004. **149**(1-3): p. 616-622.